Optical resonance tuning and polarization of thin-walled tubular microcavities

Vladimir A. Bolaños Quiñones, Gaoshan Huang, Johannes D. Plumhof, Suwit Kiravittaya, Armando Rastelli, Yongfeng Mei,* and Oliver G. Schmidt

Institute for Integrative Nanosciences, IFW Dresden, Helmholtzstrasse 20, 01069 Dresden, Germany
**Corresponding author: y.mei@ifw-dresden.de*

Received April 29, 2009; revised June 23, 2009; accepted June 25, 2009;
posted July 14, 2009 (Doc. ID 110763); published July 29, 2009

We present experimental and finite-difference time-domain simulation results on the tunability of optical resonant modes of spiral microtube cavities, rolled-up from square patterned SiO/SiO_2 thin nanomembranes on glass substrates. The peak positions of resonant TM modes shift to lower energies by coating the microtube wall with Al_2O_3 monolayers, which is well described by simulations. Moreover, a second group of tunable resonant modes appears beyond a certain critical thickness of the coated Al_2O_3. The polarization of this group of modes is TE, as we find out by a detailed analysis of the polarization-dependent photoluminescence spectra. © 2009 Optical Society of America

OCIS codes: 130.3120, 140.3945, 310.6628, 050.6875.

Optical microcavities are receiving increasing attention owing to their potential applications ranging from biosensing devices [1,2], integrated optofluidics [3], micromechanical vibration sensors [4,5], and solid-state quantum electrodynamic experiments [6]. Among different techniques used to obtain resonant optical microcavities of varying shapes and dimensions [6–10], the method of releasing and rolling up strained nanomembranes on polymers [11] allows a cheap and easy way to fabricate tubular optical cavities of various materials with deterministic diameters of a few micrometers and nanoscale wall thicknesses. These cavities have been shown to bear optical resonant modes in the visible [11,12] and infrared range [10], where the wavelengths of the modes are much larger than the tube wall thickness. However, there have been a few reports about the dependence of optical resonant modes on the wall thickness of hundred nanometers or less [10–12]. Rolled-up microtubes, characterized by thin walls and hollow geometry, may find applications as refractometers [13] for bioanalytic on-chip devices [14,15] or optofluidic microlasers [16]. This is due to a wall that is generally thinner than the wavelength [17], resulting in the inner medium strongly interacting with the evanescent field. Yang *et al.* recently showed that post-fabrication tuning of the resonant modes of silicon photonic crystal microcavities can be achieved by atomic layer deposition (ALD) [18]. This method forwards a promising way to tune the optical modes of rolled-up microtubular cavities with varying wall thickness.

In this Letter we investigate a method to tune the spectral positions of the resonant modes from thin-walled rolled-up microtubes on a glass substrate. Stepwise one-by-one monolayer (ML) coating with Al_2O_3 by ALD leads to a controllable shift of the resonant TM modes [19] to longer wavelengths. Finite-difference time-domain (FDTD) simulations match well the observed behavior. Additional TE modes are observed for Al_2O_3 coatings thicker than approximately 20 nm, as revealed by linear polarization analysis of the emitted light.

SiO and SiO_2 bilayer nanomembranes are deposited with a thickness ratio of 1:4 onto a patterned photoresist (used as a sacrificial layer) on glass substrates, following a fabrication method previously described in detail [11,14]. Microtubes are uniformly coated with Al_2O_3 using ALD (Savannah 100, Cambridge NanoTech Inc.) One monolayer of Al_2O_3 coated by ALD at 80 °C is approximately 0.9 Å in thickness, which is calibrated by atomic force microscope (AFM, Digital Instruments DI3100). The optical properties are investigated by micro photoluminescence (μ-PL) spectroscopy at room temperature [13,14].

The tube diameter can be tuned by changing the layer thickness and strain [11], while the number of rotations of the nanomembranes can be controlled by predefining the size and shape of the sacrificial layer [14]. We employed square patterned shapes [see scanning electron microscopy (SEM) image in the lower right inset of Fig. 1(a)] and an angled deposition method [11]. The microtubes can be fabricated on a large variety of planar substrates such as glass [see upper inset of Fig. 1(a)]. Because of the transparency of glass, these microtubes can be directly used in biological analysis systems [15]. The microtube diameter increases with increasing thickness of the SiO/SiO_2 bilayer t [Fig 1(a)] [11]. Since light leakage losses are expected to increase with decreasing t, we carried out PL measurements on rolled-up tubes with different diameters, to determine the lower limit of t, for which resonant modes can still be observed. Figure 1(b) displays four typical spectra collected from tubes with t and diameters indicated in Fig. 1(a). When t increases, the resonant modes become more pronounced and the free spectral range (FSR) decreases. On the contrary, when the tube wall is reduced, light diffraction can dominate the mode propagation in the tube wall, leading to the light confinement and corresponding resonant modes becoming practically unobservable. In our case, we can only see very weak modes when the layer thickness of the rolled-up tube is thinner than 27 nm.

We now focus on a tube rolled-up from a layer with $t \sim 39$ nm (noted as III in Fig. 1) and a diameter of

0146-9592/09/152345-3/$15.00

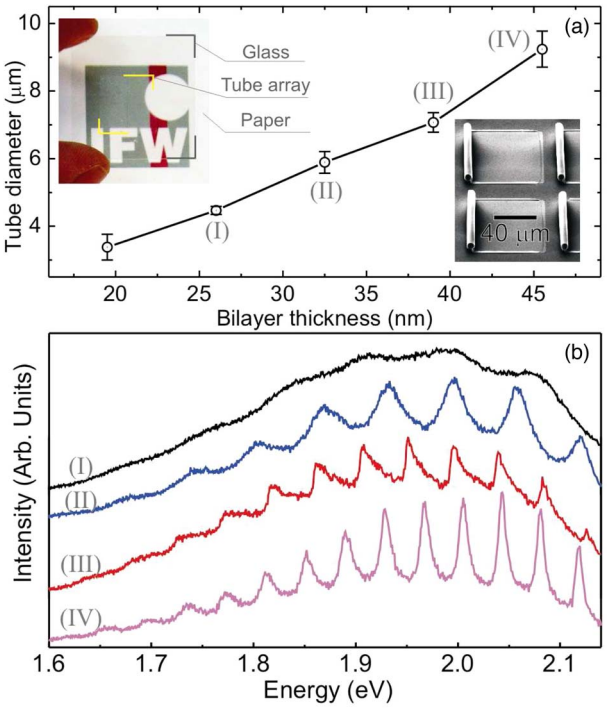

Fig. 1. (Color online) (a) Microtube diameter as a function of thickness t of SiO/SiO_2 bilayer nanomembranes. The upper inset shows a rolled-up microtubular cavity array fabricated on a transparent glass substrate. The lower inset shows an SEM image of microtubes rolled up from a square pattern. (b) PL spectra for various microtubes (i.e., different wall thicknesses) from (a).

about 7 μm to study the dependence of mode spectral position on the wall thickness, which is controlled by Al_2O_3 ML-by-ML coating using ALD. A cross-sectional view of a spiral microtube before and after ALD coating is schematically shown in Fig. 2(a), which indicates that the deposited material is coated on both the inner and outer surfaces of the tube. We measure the PL spectra at the same point on the microtube after each coating step, shown in Fig. 2(b). The shift of optical modes to lower energies is labeled by the solid circular and empty triangular markers. We see that the mode positions can be smoothly shifted (see also Fig. 3) over a wide spectral range, larger than the FSR; demonstrating that ALD of Al_2O_3 can be used to coarse and fine tune the properties of optical resonators after their fabrication. After 210 ML coating, new shoulder peaks start to be resolved [see filled triangle markers in Fig. 2(b)], exhibiting also a simultaneous energy shift, which we will discuss later.

In Fig. 3(a), we show a series of PL spectra of the microtube with Al_2O_3 coatings of up to 100 ML (the normalized peak intensity is color coded). An average redshift of 33 meV is clearly measured for all modes. We observe that modes with lower energy present a slightly smaller absolute energy shift. For instance, the modes initially located at 1.86 (2.08) eV shift by 31.6 (35.1) meV after coating with 100 ML Al_2O_3. This effect can be deducted from the resonance condition $n_{\text{eff}}l=\lambda m$, where n_{eff} is the effective refractive index of the tube wall, l is the tube circumference, m

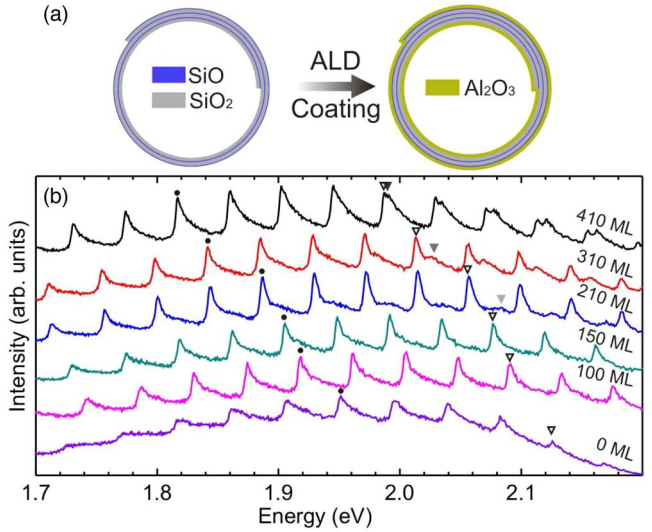

Fig. 2. (Color online) (a) Schematic cross-section diagram of an SiO/SiO_2 microtube before and after ALD coating with Al_2O_3. (b) PL spectra from the center of an ~7 μm diameter tube after coating with Al_2O_3 layers with increasing thicknesses (in MLs). Symbols mark the evolution of two TM modes (solid circles and empty triangles) and one TE mode (solid triangles).

is the azimuthal mode number, and λ is the wavelength corresponding to the mode number [10]. The differential between the energy and the effective refractive index, that is, the change of peak energy after coating the microtube, can be calculated as $dE/dn_{\text{eff}}=-E/n_{\text{eff}}$. In agreement with the experimental results in Fig. 3(a), we obtain a negative slope (decrease of E for increasing n_{eff}) and observe that higher energy modes display a larger absolute shift with the same coating thickness (i.e., the change of n_{eff}.) The physical meaning of this larger shift can be qualitatively understood if we note that a higher-energy mode corresponds to a larger m (i.e., more nodes for the corresponding resonant mode) [17] and thus is more influenced by the Al_2O_3 coating.

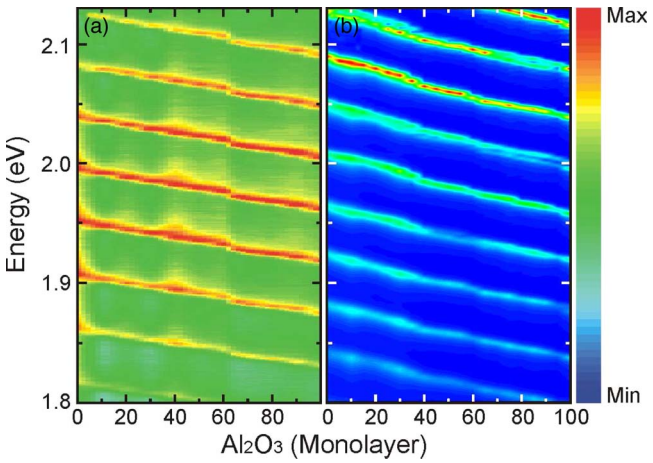

Fig. 3. (Color online) (a) Color-coded normalized peak intensity of PL spectra showing the energy shift for the resonant modes from a microtube of 7 μm in diameter coated with Al_2O_3 up to 100 MLs. (b) FDTD simulations for the actual tube in (a) for the energy shift of the resonant modes as a function of the number of ML coatings.

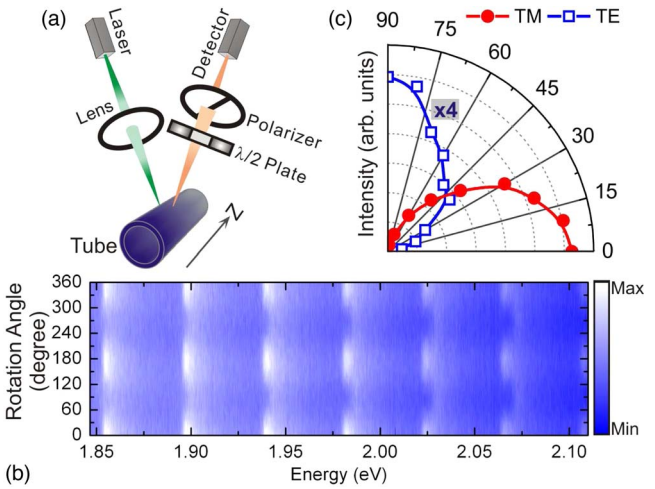

Fig. 4. (Color online) (a) Schematic diagram of the PL setup for polarization measurement. (b) PL intensity map as a function of polarization angle with respect to the tube axis direction (0°). (c) Average PL peak-to-valley intensity ratio as a function of the polarization angle for the two peaks around 2.07 eV in Fig. 4(b); the TE mode intensity has been amplified four times for the sake of clarity.

Figure 3(b) shows the results of FDTD simulations (Lumerical Solutions software) performed to reveal the resonant mode shifts using the same dimensions of the actual tube [14]. Because of lower diffraction and known polarization geometry [17], a TM-polarized source is used for simulation. Refractive indices of SiO_2, SiO, and Al_2O_3 measured by ellipsometry are 1.45, 1.55, and 1.63, respectively, and are used as input parameters in our FDTD simulation. A satisfactory agreement is obtained between simulation and experiment, which well reproduces the redshift of the modes, as presented in Fig. 3.

Finally, we discuss the shoulder peaks in Fig. 2(b) (filled triangles). Since previous results attribute the resonant modes to strongly linearly polarized light along the tube axis (TM modes) [10,12], we performed polarization-dependent PL measurements by means of a rotating achromatic lambda half-wave plate and a fixed Glan–Thompson polarizer placed in front of the spectrometer [see diagram in Fig. 4(a)]. The obtained results are shown as a color-coded intensity map in Fig. 4(b), where 0°/90° indicate light emission linearly polarized parallel/perpendicular to the tube axis. We see that the spectra in Fig. 4(b) resolve the shoulder peaks at 90°, while the main peaks are remarkably suppressed. Figure 4(c) shows the average PL peak-to-valley ratio as a function of the rotation angle for the two selected peaks around 2.07 eV in Fig. 4(b). The main peak has a maximal intensity at 0° and a minimal intensity at 90°, while the shoulder peak shows the opposite behavior. Thus, the two groups of peaks can be assigned as TM and TE modes owing to their perpendicular polarization. As expected, the large diffraction loss of TE modes [14] is reduced when the tube wall becomes thicker, allowing the microresonator to simultaneously support both TE and TM modes.

In summary, we fabricated microtubular resonators on glass substrate by releasing prestressed silicon oxide bilayer structures and found that the tube diameter is directly controlled by altering the thickness of nanomembranes. The spectral position and polarization of the modes can be smoothly tuned in a wide spectral range by Al_2O_3 coating, which can be well described by FDTD calculations. The fine tunability, which is essential for realizing optical microdevices, brings a better understanding of the resonant modes in microtubular cavities, suggesting that the microtubes could be used in potential applications for on-chip components like filters and sensors.

This work is financially supported by the Volkswagen Foundation (I/84 072). The authors thank Juliane Gabel, Ronny Engelhard, Mohamed Benyoucef, and Emica Coric for experimental assistance and Elliot John Smith for fruitful discussion.

References

1. F. Vollmer and S. Arnold, Nat. Methods **5**, 591 (2008).
2. A. M. Armani, R. P. Kulkarni, S. E. Fraser, R. C. Flagan, and K. J. Vahala, Science **317**, 783 (2007).
3. C. Monat, P. Domachuk, and B. J. Eggleton, Nat. Photonics **1**, 106 (2007).
4. A. Schliesser, G. Anetsberger, R. Rivière, O. Arcizet, and T. J. Kippenberg, New J. Phys. **10**, 095015 (2008).
5. G. Anetsberger, R. Rivière, A. Schliesser, and T. J. Kippenberg, Nat. Photonics **2**, 627 (2008).
6. K. Srinivasan and O. Painter, Nature **450**, 862 (2007).
7. D. K. Armani, T. J. Kippenberg, S. M. Spillane, and K. J. Vahala, Nature **421**, 925 (2003).
8. T. J. Kippenberg, S. M. Spillane, D. K. Armani, and K. J. Vahala, Appl. Phys. Lett. **83**, 797 (2003).
9. S. M. Spillane, T. J. Kippenberg, and K. J. Vahala, Nature **415**, 621 (2002).
10. T. Kipp, H. Welsch, Ch. Strelow, Ch. Heyn, and D. Heitmann, Phys. Rev. Lett. **96**, 077403 (2006).
11. Y. F. Mei, G. S. Huang, A. A. Solovev, E. Bermúdez Ureña, I. Mönch, F. Ding, T. Reindl, R. K. Y. Fu, P. K. Chu, and O. G. Schmidt, Adv. Mater. **20**, 4085 (2008).
12. R. Songmuang, A. Rastelli, S. Mendach, and O. G. Schmidt, Appl. Phys. Lett. **90**, 091905 (2007).
13. A. Bernardi, S. Kiravittaya, A. Rastelli, R. Songmuang, D. J. Thurmer, M. Benyoucef, and O. G. Schmidt, Appl. Phys. Lett. **93**, 094106 (2008).
14. G. S. Huang, S. Kiravittaya, V. A. Bolaños Quiñones, F. Ding, M. Benyoucef, A. Rastelli, Y. F. Mei, and O. G. Schmidt, Appl. Phys. Lett. **94**, 141901 (2009).
15. G. S. Huang, Y. F. Mei, D. J. Thurmer, E. Coric, and O. G. Schmidt, Lab Chip **9**, 263 (2009).
16. H. J. Moon, Y. T. Chough, and K. An, Phys. Rev. Lett. **85**, 3161 (2000).
17. M. Hosoda and T. Shigaki, Appl. Phys. Lett. **90**, 181107 (2007).
18. X. D. Yang, C. J. Chen, C. A. Husko, and C. W. Wong, Appl. Phys. Lett. **91**, 161114 (2007).
19. See the definition in [17].